

International Journal of Physical Sciences

Volume 11 Number 5 16 March 2016

ISSN 1992-1950

Normal P axis, PR, rate & rhythm
P V1 < 10 mV or more negative
QIS in V1 & V2
QTc > 470 ms
ST-T negative ANTILAT/MP
T > -30 mV, ST > -05 mV



*Academic
Journals*

ABOUT IJPS

The **International Journal of Physical Sciences (IJPS)** is published weekly (one volume per year) by Academic Journals.

International Journal of Physical Sciences (IJPS) is an open access journal that publishes high-quality solicited and unsolicited articles, in English, in all Physics and chemistry including artificial intelligence, neural processing, nuclear and particle physics, geophysics, physics in medicine and biology, plasma physics, semiconductor science and technology, wireless and optical communications, materials science, energy and fuels, environmental science and technology, combinatorial chemistry, natural products, molecular therapeutics, geochemistry, cement and concrete research, metallurgy, crystallography and computer-aided materials design. All articles published in IJPS are peer-reviewed.

Contact Us

Editorial Office: ijps@academicjournals.org

Help Desk: helpdesk@academicjournals.org

Website: <http://www.academicjournals.org/journal/IJPS>

Submit manuscript online <http://ms.academicjournals.me/>

Editors

Prof. Sanjay Misra

*Department of Computer Engineering, School of Information and Communication Technology
Federal University of Technology, Minna,
Nigeria.*

Prof. Songjun Li

*School of Materials Science and Engineering,
Jiangsu University,
Zhenjiang,
China*

Dr. G. Suresh Kumar

*Senior Scientist and Head Biophysical Chemistry
Division Indian Institute of Chemical Biology
(IICB)(CSIR, Govt. of India),
Kolkata 700 032,
INDIA.*

Dr. Remi Adewumi Oluyinka

*Senior Lecturer,
School of Computer Science
Westville Campus
University of KwaZulu-Natal
Private Bag X54001
Durban 4000
South Africa.*

Prof. Hyo Choi

*Graduate School
Gangneung-Wonju National University
Gangneung,
Gangwondo 210-702, Korea*

Prof. Kui Yu Zhang

*Laboratoire de Microscopies et d'Etude de
Nanostructures (LMEN)
Département de Physique, Université de Reims,
B.P. 1039. 51687,
Reims cedex,
France.*

Prof. R. Vittal

*Research Professor,
Department of Chemistry and Molecular
Engineering
Korea University, Seoul 136-701,
Korea.*

Prof Mohamed Bououdina

*Director of the Nanotechnology Centre
University of Bahrain
PO Box 32038,
Kingdom of Bahrain*

Prof. Geoffrey Mitchell

*School of Mathematics,
Meteorology and Physics
Centre for Advanced Microscopy
University of Reading Whiteknights,
Reading RG6 6AF
United Kingdom.*

Prof. Xiao-Li Yang

*School of Civil Engineering,
Central South University,
Hunan 410075,
China*

Dr. Sushil Kumar

*Geophysics Group,
Wadia Institute of Himalayan Geology,
P.B. No. 74 Dehra Dun - 248001(UC)
India.*

Prof. Suleyman KORKUT

*Duzce University
Faculty of Forestry
Department of Forest Industrial Engineering
Beciyorukler Campus 81620
Duzce-Turkey*

Prof. Nazmul Islam

*Department of Basic Sciences &
Humanities/Chemistry,
Techno Global-Balurghat, Mangalpur, Near District
Jail P.O: Beltalpark, P.S: Balurghat, Dist.: South
Dinajpur,
Pin: 733103,India.*

Prof. Dr. Ismail Musirin

*Centre for Electrical Power Engineering Studies
(CEPES), Faculty of Electrical Engineering, Universiti
Teknologi Mara,
40450 Shah Alam,
Selangor, Malaysia*

Prof. Mohamed A. Amr

*Nuclear Physic Department, Atomic Energy Authority
Cairo 13759,
Egypt.*

Dr. Armin Shams

*Artificial Intelligence Group,
Computer Science Department,
The University of Manchester.*

Editorial Board

Prof. Salah M. El-Sayed

*Mathematics. Department of Scientific Computing,
Faculty of Computers and Informatics,
Benha University. Benha ,
Egypt.*

Dr. Rowdra Ghatak

*Associate Professor
Electronics and Communication Engineering Dept.,
National Institute of Technology Durgapur
Durgapur West Bengal*

Prof. Fong-Gong Wu

*College of Planning and Design, National Cheng Kung
University
Taiwan*

Dr. Abha Mishra.

*Senior Research Specialist & Affiliated Faculty.
Thailand*

Dr. Madad Khan

*Head
Department of Mathematics
COMSATS University of Science and Technology
Abbottabad, Pakistan*

Prof. Yuan-Shyi Peter Chiu

*Department of Industrial Engineering & Management
Chaoyang University of Technology
Taichung, Taiwan*

Dr. M. R. Pahlavani,

*Head, Department of Nuclear physics,
Mazandaran University,
Babolsar-Iran*

Dr. Subir Das,

*Department of Applied Mathematics,
Institute of Technology, Banaras Hindu University,
Varanasi*

Dr. Anna Oleksy

*Department of Chemistry
University of Gothenburg
Gothenburg,
Sweden*

Prof. Gin-Rong Liu,

*Center for Space and Remote Sensing Research
National Central University, Chung-Li,
Taiwan 32001*

Prof. Mohammed H. T. Qari

*Department of Structural geology and remote sensing
Faculty of Earth Sciences
King Abdulaziz UniversityJeddah,
Saudi Arabia*

Dr. Jyhwen Wang,

*Department of Engineering Technology and Industrial
Distribution
Department of Mechanical Engineering
Texas A&M University
College Station,*

Prof. N. V. Sastry

*Department of Chemistry
Sardar Patel University
Vallabh Vidyanagar
Gujarat, India*

Dr. Edilson Ferneda

*Graduate Program on Knowledge Management and IT,
Catholic University of Brasilia,
Brazil*

Dr. F. H. Chang

*Department of Leisure, Recreation and Tourism
Management,
Tzu Hui Institute of Technology, Pingtung 926,
Taiwan (R.O.C.)*

Prof. Annapurna P.Patil,

*Department of Computer Science and Engineering,
M.S. Ramaiah Institute of Technology, Bangalore-54,
India.*

Dr. Ricardo Martinho

*Department of Informatics Engineering, School of
Technology and Management, Polytechnic Institute of
Leiria, Rua General Norton de Matos, Apartado 4133, 2411-
901 Leiria,
Portugal.*

Dr Driss Miloud

*University of mascara / Algeria
Laboratory of Sciences and Technology of Water
Faculty of Sciences and the Technology
Department of Science and Technology
Algeria*

Prof. Bidyut Saha,

*Chemistry Department, Burdwan University, WB,
India*

ARTICLES

Space charge kinetic treatment in Langmuir probes with cylindrical geometry	60
E. Valdeblánquez and P. Martín	
Investigating H and Z geomagnetic component disturbance field in the mid-latitude	66
Okeke F. N., Okoro E. C. and Ugwu E. B. I.	

Full Length Research Paper

Space charge kinetic treatment in Langmuir probes with cylindrical geometry

E. Valdeblánquez^{1,2*} and P. Martín³

¹Universidad del Zulia, Facultad de Ingeniería, Apartado 4011-A 526, Maracaibo, Edo. Zulia, Venezuela.

²Centro de Investigación de Matemática Aplicada, Facultad de Ingeniería, Apartado 4011-A 526, Maracaibo, Edo. Zulia, Venezuela.

³Depto. de Física, Universidad de Antofagasta, Antofagasta, Chile.

Received 8 July, 2015; Accepted 29 February, 2016

In this paper, an analysis of the space charge build up in the interelectrode region of a velocity analyzer with cylindrical symmetry is performed using kinetic theory. Thus the present treatment includes temperature effects. Azimuth symmetry is also assumed. A detailed and comparative analysis, between planar and cylindrical electrodes, is carried out, showing the advantages of each kind of symmetries.

Key words: Space charge effects, Langmuir probes, velocity analyzers.

INTRODUCTION

Space charge formation is one of the main factors limiting the current obtained in the collector grid of a velocity analyzer, thermoionic diodes and other engineering devices (Langmuir, 1913, 1923; Langmuir and Blodgett, 1923; Page and Adams Jr., 1958; Braun et al., 1973; Martin and Donoso, 1989; Varney, 1982; Wheeler, 1980). This problem was first treated for plane electrodes (two grids) using fluid equations by Langmuir and Child (Langmuir, 1913, 1923; Langmuir and Blodgett, 1923), obtaining the so called Langmuir-Child current (Page and Adams Jr., 1958). Treatments using kinetic theory were developed later for planar electrodes (Braun et al., 1973; Martin and Donoso, 1989; Varney, 1982; Wheeler,

1980) and in this way the effect of temperature were also studied. A modified Langmuir-Child equation, including both temperature and relativistic effects, was also derived and studied using kinetic theory (Qian et al., 1994). The cylindrical and spherical probes have also been treated amply, beginning with the pioneer work of Bohm and Massey (1949) but there is no need to go through a long list of publications, because there are very good reviews in this theme, thus referring only to some of them (Parrot et al., 1982; Estes and Martín, 2000). Previous authors followed essentially two lines, one based in orbital theory and the other one by considering two regions in the probe plasma denoted by sheath and presheath. The important

*Corresponding author. E-mail: evaldeblanquez@fing.luz.edu.ve

PACS: 52.70.

Author(s) agree that this article remain permanently open access under the terms of the [Creative Commons Attribution License 4.0 International License](https://creativecommons.org/licenses/by/4.0/)

parameters in that analysis were the size of the orbits and the limits of each region. A weak point of most of these treatments is the precise limits of the sheath and presheath, which are not well defined. Another point is that they also usually assume that the amount of particles with “trapped orbits” is zero, which is not clearly justified for cylindrical probes. The treatment we are now presenting is very ample, and although kinetic theory is used, our results are rather simple and easy to calculate. The procedure here followed is an extension of the technique used by Martin and Donoso (1989) for plane electrodes.

The case of cylindrical and spherical electrodes has been also considered in recent works (Bohm and Massey, 1949; Parrot et al., 1982; Estes and Martín, 2000; Estes and Martín, 2000). Treatments have been also developed for cylindrical and spherical probes and other collectors in collision less plasmas, in the limit where the ratio of Debye length to probe radius vanishes (Estes and Martín, 2000). Here we will analyze in detail the space-charge formation in velocity analyzers with cylindrical grids. Numerical integration of the corresponding differential equation will be performed. Here the accuracy of the approximations we have found is not so satisfactory as in the case of plane electrodes (Martin and Donoso, 1989; Estes and Martín, 2000). Thus in order to find reliable results, it is better to use direct computer calculations of the second order non-linear differential equations coming from the Poisson equation, once the right distribution functions have been introduced. In this way, our analysis includes temperature effects. The build-up of interelectrode space charge is discussed for velocity analyzers with plane and cylindrical symmetries. The results of each geometry will be compared.

THEORETICAL ANALYSIS

The velocity analyzers with cylindrical electrodes here considered are shown in Figure 1. The discriminating grid G_2 is a hollow tube of radius C . The entrance grid G_1 (radius a) is biased to a negative potential or allowed to float with zero current. In this way most of the electrons are repelled by this grid. Therefore in the region, between the entrance (G_1) and discriminating (G_2) grids, there are not electrons, but only ions. This is the region of interest in this paper. We assume that all the ions that go through the discriminating grid are collected by the central collector, which is set up to a negative potential. The grid G_2 , of radius c , is biased to a positive potential in order to repel some of the ions, and this is called discriminating grid. Here a , ($OA = a$) and c , ($OC = c$) are the radius of the entrance and discriminating grids. The potentials V_0 and V_R of G_1 and G_2 are given and we look for the interelectrode potential between both grids as it is shown in the lower part of the figure. Here, c is chosen as the unit length, and this will also be the normalization unit for the draws in velocity analyzer with cylindrical electrodes.

The theoretical analysis is in somewhat similar to the case of plane electrodes, (Martin and Donoso, 1989).

However now the radial distance ρ replaces the distance x , and the operator ∇^2 has to be written in the corresponding cylindrical coordinates. Looking in detail the case of cylindrical symmetry, the distribution function for the coordinates ρ (radial), ϕ (angular) and z (along the axis), will be

$$f(\rho, \vec{v}) = f(\rho, v_\rho, v_\phi, v_z) = n_0 \left(\frac{m}{2\pi T} \right)^{\frac{3}{2}} \exp \left\{ - \left[\frac{1}{2} m \vec{v}^2 + qV(\rho) \right] / T \right\} \quad (1)$$

$$\vec{v}^2 = v_\rho^2 + v_\phi^2 + v_z^2 \quad (2)$$

Here the temperature is given in electron volts and the radial symmetry is considered, thus ϕ and z does not appear in the distribution function. The end effects have been also neglected. In this analysis the radial velocity is the important one, and the integration in v_ϕ and v_z can be carried out straightforward from $-\infty$ to $+\infty$ giving:

$$f_0(\rho, v_\rho) = n_0 \left(\frac{m}{2\pi T} \right)^{\frac{1}{2}} \exp \left\{ - \left[\frac{1}{2} m v_\rho^2 + qV(\rho) \right] / T \right\} \quad (3)$$

The ions with radial kinetic energy larger than qV_ρ (V_ρ maximum potential at $\rho = \rho_p$) will go through the maximum potential reaching the discriminating grid, and then they will be collected by the collector grid. The ions with radial kinetic energy lower than qV_ρ will be reflected. In this work, the entrance velocity are considered positive, this allows a simple comparison with planar electrodes. Therefore the radial velocity will be considered positive when they go toward the axial of the cylinder and negative in the other way. Now as it was explained in Equation 2 of Martin and Donoso (1989); the distribution function in the interval (c, ρ_p) , can be written as:

$$f(\rho, v_\rho) = \begin{cases} f_0(\rho, v_\rho) & \text{for } v_\rho > -v_{\rho_p}(\rho) \\ 0 & \text{for } v_\rho < -v_{\rho_p}(\rho) \end{cases} ; \quad \rho_p < \rho < a, \quad (4)$$

Where $f_0(\rho, v_\rho)$ is the one dimensional Maxwellian distribution, and V_ρ is defined by the equation:

$$\frac{1}{2} m \left[v_{\rho_p}(\rho) \right]^2 + qV(\rho) = qV_\rho. \quad (5)$$

Note that, because of the preceding definition, $v_{\rho_p}(\rho_p)$ will be zero.

Velocity analyzer with cylindrical electrodes

In the interelectrode region between the maximum potential V_ρ and the discriminating grid at $\rho=c$, there is no reflected particles, because we assume that all the ions arriving to the discriminating grid are collected by the collector. Therefore, the distribution function will be:

$$f(\rho, v_\rho) = \begin{cases} f_0(\rho, v_\rho) & \text{for } v_\rho > v_{\rho_p}(\rho) \\ 0 & \text{for } v_\rho < v_{\rho_p}(\rho) \end{cases} ; \quad c < \rho < \rho_p, \quad (6)$$

For $\rho = \rho_p$, $v_{\rho_p}(\rho_p) = 0$, and both distribution functions are coincident. Thus the continuity of the current is assured. Using now

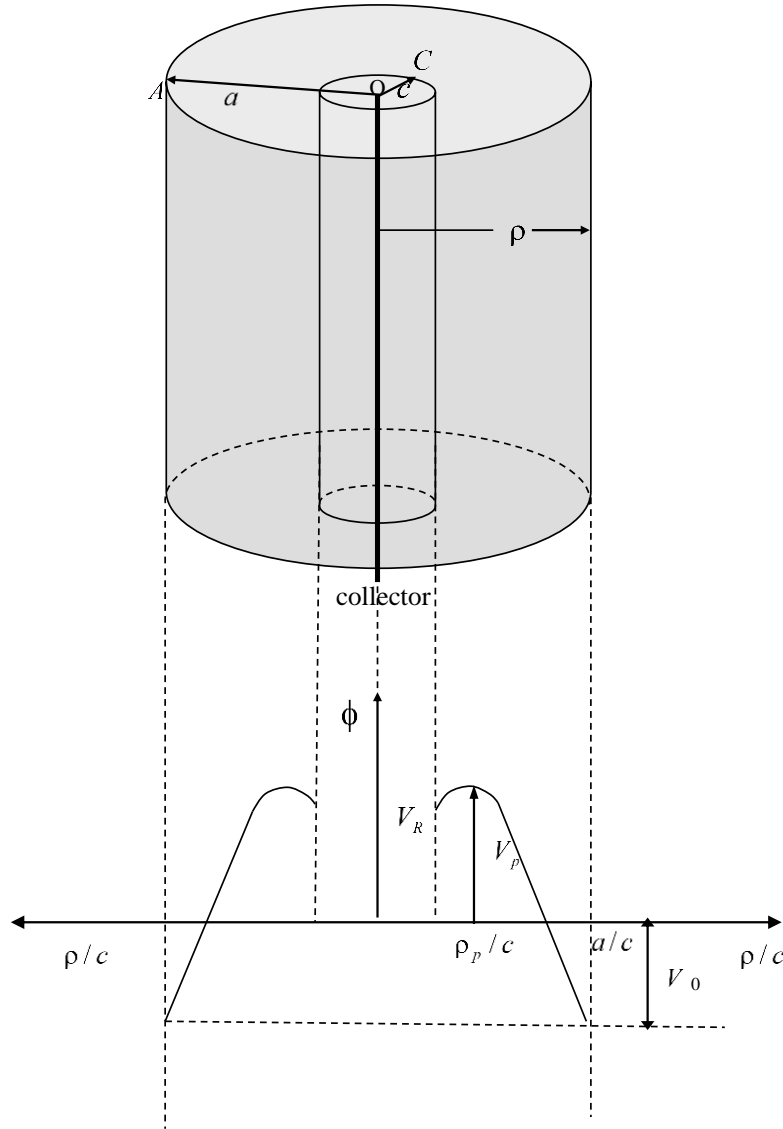


Figure 1. A velocity analyzer with cylindrical electrodes is sketched. At the lower part of the draw we show a typical potential curve.

the Debye length for ions $\lambda_D^2 = \frac{T}{4\pi n_0 e^2}$ and dimensionless variables r and ϕ :

$$r = \frac{\rho}{\lambda_D}; \phi(\rho) = q[V_p - V(\rho)]/T; r_p = \frac{\rho_p}{\lambda_D}, \tilde{c} = \frac{c}{\lambda_D}, \tilde{r} = \frac{r}{\tilde{c}} \quad (7)$$

The Poisson equation for the potentials in cylindrical coordinates with azimuthal symmetry, will be

$$\nabla^2 V(\rho) = \frac{1}{\rho} \frac{d}{d\rho} \left(\rho \frac{dV(\rho)}{d\rho} \right) = -4\pi n_i(\rho) \quad (8)$$

where n_i is the ion density. Because of the azimuthal symmetry, as well as, Z symmetry:

$$n_i(\rho) = \int_{-\infty}^{\infty} f(\rho, v_\rho) dv_\rho \quad (9)$$

Now from Equation 4, for $r_p < r < a$

$$n_i(\rho) = \int_{-\infty}^{\infty} f(\rho, v_\rho) dv_\rho = \int_{-v_{\rho p}}^{\infty} f_0(\rho, v_\rho) dv_\rho \quad (10)$$

Using the new variable y , defined as

$$y^2 = \frac{\frac{1}{2}mv_\rho^2}{T}, y_p^2 = \frac{\frac{1}{2}mv_{\rho p}^2}{T} = q \frac{[V_p - V(\rho)]}{T} = \phi, \phi_p = \frac{qV_p}{T} \quad (11)$$

then

$$n_i(\rho) = \frac{n_0}{\sqrt{\pi}} \exp \left[-\frac{qV(\rho)}{T} \right] \int_{-y_p}^{\infty} \exp(-y^2) dy \quad (12)$$

$$n_i(\rho) = \frac{n_0}{\sqrt{\pi}} \exp \left(\phi_p - \phi(\rho) \right) \int_{-\sqrt{\phi(\rho)}}^{\infty} \exp(-y^2) dy \quad (13)$$

$$n_i(\rho) = \frac{n_0}{\sqrt{\pi}} \exp(\phi_p - \phi(\rho)) \left\{ \int_{-\sqrt{\phi(\rho)}}^0 \exp(-y^2) dy + \int_0^{\infty} \exp(-y^2) dy \right\} \quad (14)$$

$$n_i(\rho) = \frac{n_0}{\sqrt{\pi}} \exp(\phi_p - \phi(\rho)) \left[\int_0^{\sqrt{\phi(\rho)}} \exp(-y^2) dy + \int_0^{\infty} \exp(-y^2) dy \right] \quad (15)$$

$$n_i(\rho) = \frac{n_0}{2} \exp(\phi_p - \phi(\rho)) \left[1 + \operatorname{erf}\left(\phi^{\frac{1}{2}}\right) \right] \quad (16)$$

Where $\operatorname{erf}\left(\phi^{\frac{1}{2}}\right)$ is the error function of $\phi^{\frac{1}{2}}$.

The Poisson equation in dimensionless variables becomes:

$$\frac{1}{r} \frac{d}{dr} \left(r \frac{d\phi(r)}{dr} \right) = \frac{1}{2} \exp(\phi_p - \phi(r)) \left[1 + \operatorname{erf}\left(\phi^{\frac{1}{2}}\right) \right] \quad (17)$$

for $r_p < r < \frac{a}{\lambda_D}$.

The case of $\frac{c}{\lambda_D} < r < r_p$ is analyzed in the same way, but it appears now the sign minus on the error function, resulting:

$$\frac{1}{r} \frac{d}{dr} \left(r \frac{d\phi(r)}{dr} \right) = \frac{1}{2} \exp(\phi_p - \phi(r)) \left[1 \pm \operatorname{erf}\left(\phi^{\frac{1}{2}}\right) \right] \quad (18)$$

Where the + sign is for the region near the entrance grid, and the - sign is for the region near the discriminating grid. A first integration of Equation 18 cannot be performed, which is different to the planar case, where a first integration was done and a most simple first order equation was obtained (Martin and Donoso, 1989).

RESULTS

The integration of Equation 18 has been carried out using fourth order Runge-Kutta algorithm. The analysis is simplified, if we give the values of ϕ_p and ρ_p , and the potentials V_0 and V_R , corresponding to ϕ_0 and ϕ_R , are determined from ϕ_p and ρ_p .

In Figures 2 and 3, the interelectrode potential for cylindrical and plane velocity analyzers are shown. The procedure here found more convenient, is to give values to the maximum potential ϕ_p as well as the position and to determine all the other values from these quantities. In Figure 2, the same values than in Figure 3 are used for ϕ_p and the position of the maximum, but the analysis is performed for electrodes with cylindrical symmetry, instead of a plane one. The scale factor potential in Figure 2 is double than in Figure 3. For $\rho_p = 1$, the entrance grid voltage is -3.8 volts ($\rho/c=5$) in Figure 2, compared with -1.4 volts in Figure 3. In the case of planar electrodes, the repelling of electrons is more efficient than in the case of cylindrical electrodes. For $\phi_p = 0.75$,

$\left(\phi_p = \frac{qV_p}{T} \right)$, the buildup of space charge begins when ϕ_a

$= -1.4 \left(\phi_a = \frac{qV_a}{T} \right)$ for planar electrodes, compared with

$\phi_a = -3.8$ for cylindrical symmetries. One advantage of cylindrical electrodes is that the current can be increased easily using longer electrodes. In Figure 3, we show the case of planar electrodes for the corresponding values of $\phi_p = 0.75$ and $x_p = (0, 0.5, 1, 1.5, 2, 2.5, 3, 3.5, 4)$. Now the interelectrode distance is measured from the discriminating electrode instead of the central axis. Thus this interelectrode distance goes from zero to four, instead of one to five as in previous case, and the values are one unit smaller. The same phenomena, that happened when we move from cylindrical to planar electrodes, happens now, that is, for $\phi_R = 0.75$, the absolute charge effect begins when $\phi_a = -1.42$ for planar electrodes. This value is smaller than the absolute value of ϕ_a ($\phi_a = -3.8$) in the case of cylindrical electrodes.

Therefore using planar electrodes there is a better repelling of electrons. The advantage of using cylindrical electrodes could be in the facility of increasing the collector current by increasing the length of the cylinder. Furthermore the plasma disturbing, because of introduction of a probe, could be less important in this case. We want to point out that the distances in Figures 2 and 3, cannot be compared well, because the unit in Figure 3, λ_D , instead of the radius c of the discriminating grid in Figure 2.

When ϕ_p changes, there is also changes in the pattern of the characteristics curves. In Figure 4, we have $\phi_p = 0.65$, and the same values than in Figure 2 for \tilde{r}_p ($\tilde{r}_p = 1, 1.5, 2, 2.5, \text{ and } 3$). Comparing with Figure 2, ϕ_p has been decreased by a factor 0.15. However ϕ_a is now -12.4 for $\tilde{r}_p = 1$, that is, ϕ_p decreases by a smaller factor.

Conclusion

In this paper space charge effects in velocity analyzers for cylindrical geometries, using kinetic theory, and therefore including temperature effects, have been analyzed. Our analysis shows that the repelling of the electrons is more effective for planar electrodes than for cylindrical geometries. This kind of velocity analyzers seems appropriated to be installed in space ships to characterize the outside plasmas. The advantage of cylindrical grids with respect to planar ones could be in the facility to collect larger currents with a less plasma disturbance. The equations here presented include temperature effects, since kinetic theory is used to determine them. However, no simple equation has been

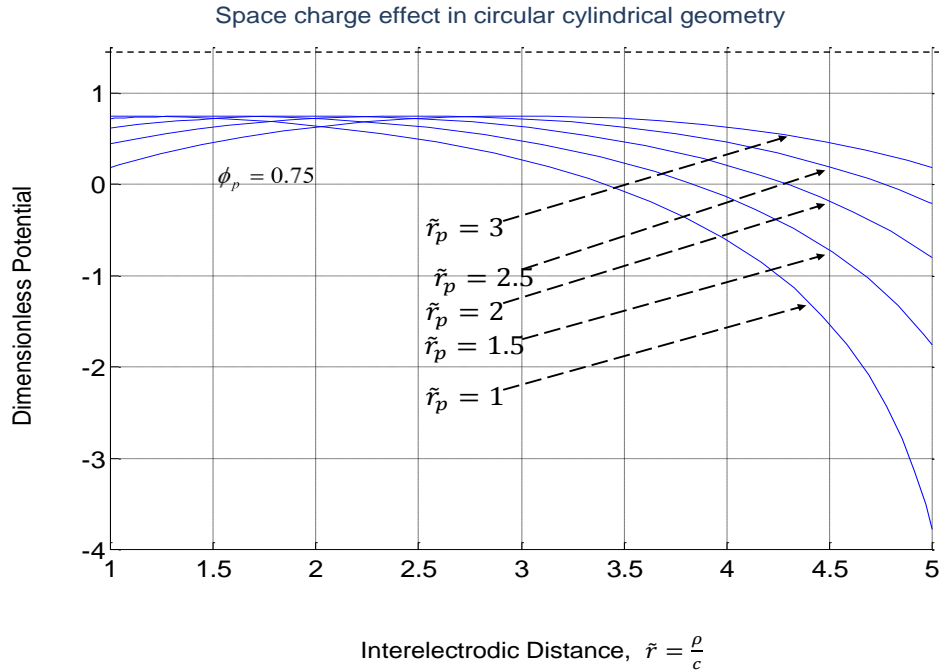


Figure 2. Interelectrode potentials in a cylindrical velocity analyzer. Numerical calculations were performed keeping the same interelectrode distance and changing the potentials in the electrodes. In the actual calculations the procedure was to give the value of the maximum $\phi_p = 0.75$ and taking five different values for the position maximum positions $\rho_p / c = 1, 1.5, 2, 2.5$ and 3 .

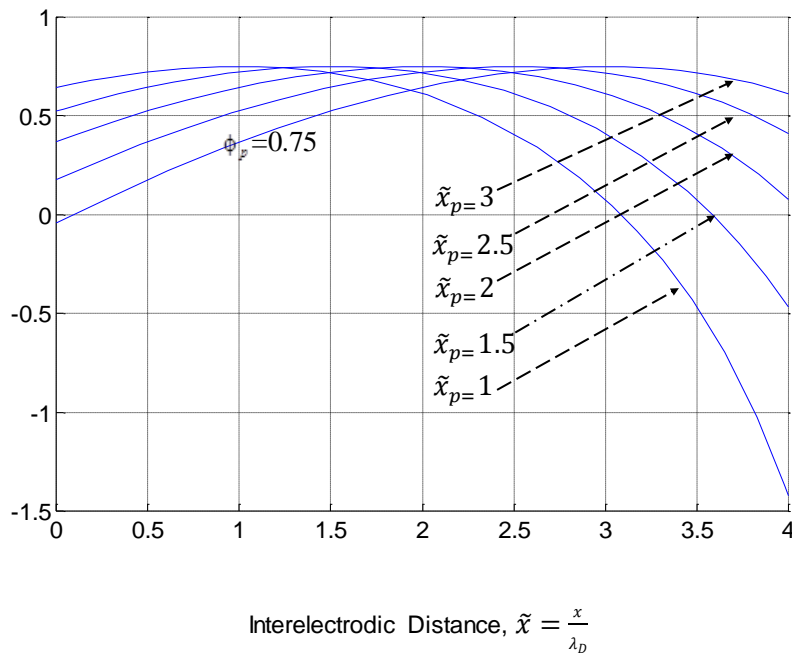


Figure 3. Interelectrode potentials in a plane velocity analyzer for a maximum potential $\phi_p = 0.75$ and the same conditions than in the case of cylindrical geometry. Now the positions are $x / \lambda_D = 0, 0.5, 1, 1.5, 2, 2.5$ and 3 . And the entrance potentials are equal.

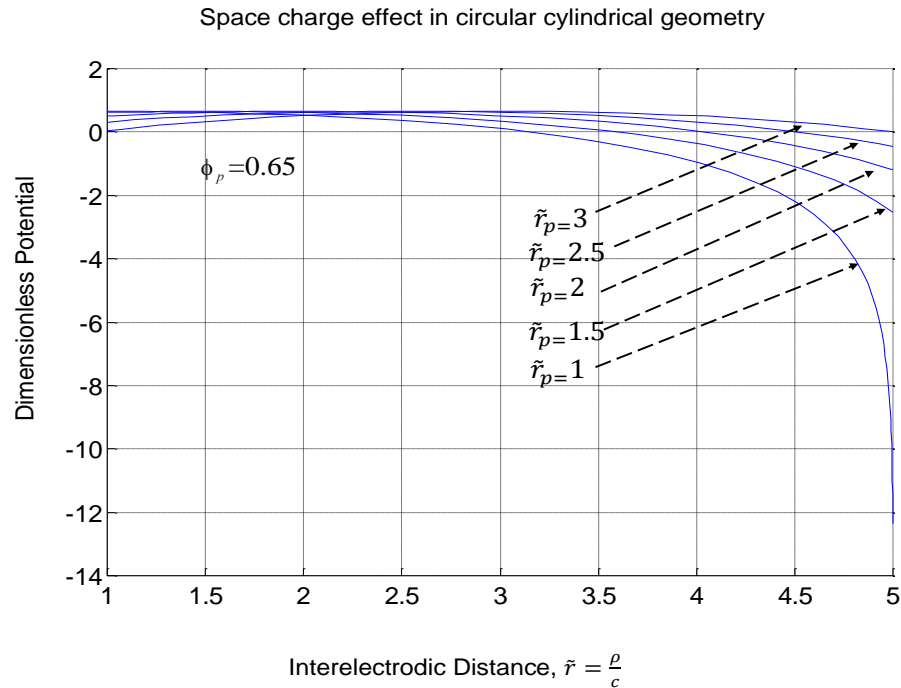


Figure 4. Interelectrode potentials in a cylindrical velocity analyzer. Similar as in figure 2; that is, keeping the same maximum potentials positions $\rho_p / c = 1, 1.5, 2, 2.5$ and 3, but changing the value of the maximum to $\phi_p = 0.65$.

found for the electric current, for instance, similar to Equation 29 in Martin and Donoso (1989) for planar electrodes, generalizing the Langmuir Child current. Here the problem is more complicated, since no first integration of Poisson equation can be performed, as it was done in Martin and Donoso (1989).

Conflict of interests

The authors have not declared any conflict of interests.

ACKNOWLEDGEMENTS

This work was supported by research project from CONDES, Universidad del Zulia, Maracaibo, Venezuela, and grants DID G22, Universidad Simón Bolívar, Caracas, Venezuela and Proyecto ANT 128, programa Mecesus, Universidad de Antofagasta, Chile.

REFERENCES

Bohm D, Burhop EHS, Massey HSW (1949). Characteristics of electrical Discharges in Magnetic Field. Edited by Guthrie A, Wakerling RK (McGraw-Hill, New York, 1949) Chap. 2. pp. 13-76.

- Braun JC, Richard M, Felden M (1973). Détermination de la répartition de potentiel dans l'espace interélectrode d'une sonde à grille plongée dans un plasma maxwellien. *J. Phys.* 34:859-867.
- Estes RD, San Martín JR (2000). Cylindrical Langmuir probes beyond the orbital-motion-limited regime. *Phys. Plasmas* 7:432.
- Langmuir I (1913). The Effect of Space Charge and Residual Gases on Thermionic Currents in High Vacuum. *Phys. Rev.* 2:450-486.
- Langmuir I (1923). The Effect of Space Charge and Initial Velocities on the Potential Distribution and Thermionic Current between Parallel Plane Electrodes. *Phys. Rev.* 21:419-435.
- Langmuir I and Blodgett K (1923). Currents Limited by Space Charge between Coaxial Cylinders. *Phys. Rev.* 22:347-356.
- Martin P, Donoso G (1989). A new Langmuir-Child equation including temperature effects. *Phys. Fluids B* 1:247.
- Page L, Adams NI Jr. (1958). Principles of Electricity (New York: Van Nostrand, Englewood Cliffs, NJ, 1958), 3rd ed. P 253.
- Parrot MJM, Storey LRO, Parker LW, Laframboise JG (1982). Theory of cylindrical and spherical Langmuir probes in the limit of vanishing Debye number. *Phys. Fluids* 25:2388.
- Qian B-L, Liu Y-G, Li C-L (1994). Both temperature and relativistic effects on the Langmuir Child equation. *Phys. Plasma* 7:2398.
- Varney RN (1982). Falsification by space charge of electron beam energy measurements. *Am. J. Phys.* 49:425.
- Wheeler CB (1980). Space-charge-limited current flow between plane-parallel electrodes in a low-density gas. *J. Phys. A* 13:1873.

Full Length Research Paper

Investigating H and Z geomagnetic component disturbance field in the mid-latitude

Okeke F. N., Okoro E. C.* and Ugwu E. B. I.

Department of Physics and Astronomy, University of Nigeria, Nsukka, Nigeria.

Received 23 October, 2015; Accepted 15 February, 2016

The relationship in the variations of geomagnetic horizontal component (H) and vertical component (Z) in Boulder station (40.1°N, 254.8°) has been investigated. In the analysis, series of significant changes in amplitude and period are observed in H as well as in Z during the day-time. The changes in H and Z for the average yearly diurnal variations and for the monthly variations do not exhibit consistent similar pattern for the years under study. The variations in H component of the field exhibit no significant peak around noon as should have been expected. The H component peak is observed to be positive throughout the period of study. The Z component variation was nearly mostly negative for all the years. Cause of these variations is expected to have arisen largely from different sources, either external or internal. It therefore seems that variations in H and Z component fields in mid-latitude as compared to those in equatorial electrojet regions are in contrast. The reason is attributed to the fact that cause of variation in equatorial electrojet (EEJ) regions emanate from the same source, while that in the mid-latitude emanate from different source.

Key words: Geomagnetic components, mid-latitude, disturbance field, variations, electrojet.

INTRODUCTION

Vonlland and Taubenheim (1958), made a very crucial discovery that magnetic intensity decreases with latitude. Bhargava and Yacob (1971) had shown that increasing values of geomagnetic disturbance index, A_p , are associated with increasing values of daily means of geomagnetic field. Sarabhai and Nair (1969) had earlier suggested that the daily variation of the horizontal intensity at a low latitude station, outside the effect of EEJ is due to a decrease of the ambient field on the night side rather than an increase during the day time.

It is important to note that the disturbance daily variation SD, which depends on local time, is not a

constant intensity but could decrease from the first to the second day of the storm. Its variation is also very different from that of S_q , both in times of max and min and in relation to latitude. One of the most striking features of the characteristics of the D- field is the increasing predominance of the SD part of the field as compared with the Dst part, when auroral zone is being approached from the low latitudes.

It has earlier been observed that for middle and low latitudes, S_q variation is greatest during the day hours having a sharp peak shortly before noon. In contrast, SD variation is mainly diurnal with an early morning peak.

*Corresponding author. E-mail: eucharia.okoro@unn.edu.ng. Tel: +234-803 333 4279.

In the past, Vestine (1947) attributed ionospheric current systems of appropriate forms and strength.

Onwumechili (1959) studied the relation between H- and Z- component variation near equatorial electrojet station. In his study, it was found that H and Z both increase and decrease together; it was concluded that these variations in both H and Z could arise from the same cause; hence they have much in common.

Work of Fambitakoye (1971) gave the first latitudinal profile of dH and dZ due to normal and counter electrojet events using nine equatorial stations in central Africa.

Rastogi (2006) found that during heavy storm, variations in H field component near the earth surface are higher at stations closer to magnetic equator. He attributed the cause of the special storm time effect to additional westward electric field imposed due to the interaction of solar wind with interplanetary magnetic field (IMF).

Okeke and Hamano (2000) found that the amplitude of dH has diurnal variation which peaks during the day at about local noon in all the three EEJ regions, which they attributed to the enhanced dynamo action at these three stations.

Messanga et al. (2014) examined the variability of H component of geomagnetic field in Central African sector provided by Yaounde Cameroon Amber. It was found that the scattering of H component of magnetic field variation is more on disturbed than that on quiet condition.

Jean-Louis et al. (2013) investigated solar events through geomagnetic activities and physical processes on the sun. Their results confirm the classification scheme that quiet activity reflects slow wind effects, while recurrent activity effects reflects high wind stream and unclear activity answers to the fluctuations between high wind stream and slow wind effects. From available literature, it is obvious that much work has been carried out on H, Z in connection with EEJ zones, while little attention has been given to H and Z in mid-latitude. Hence, it becomes pertinent that this study be carried out so as to compare the variations in H and Z geomagnetic components in mid-latitude with those in EEJ zones.

Sources of data

The geomagnetic field data for Boulder Colorado (40.1°N, 254.8°E), was obtained from World Data Center (WDC) for geomagnetism, Kyoto, Japan. The disturbed days for the disturbance field variation were selected as the five most disturbed days of each month for the nine years (1990 – 1998), employed in this study.

METHODS OF ANALYSIS

The nine years diurnal variations were computed using MatLab software. The average of the hours of the five most disturbed days of each month was equally computed, this yields the monthly

disturbance field values. Tables 1, 2 and 3 depict S_d variations of H component, S_d variations for the Z components and average monthly S_d variation for H and Z components for the year 1990 to 1998. The base line is defined as:

$$H_o = (H_1 + H_2 + H_{23} + H_{24})/4 \quad (1)$$

Where H_1, H_2, H_3 and H_{24} are the four hours flanking local mid night.

The amplitude of the hourly variation is given by:

$$\Delta H_{s_d} = (H_i - H_o) \quad (2)$$

Where H_i is the i th hour of H –component value.

Then, the Z- component variation is given by:

$$\Delta Z_{s_d} = (Z_i - Z_o) \quad (3)$$

Where Z_o and Z_i are the base line values for each month and i th hour value respectively.

The disturbed value is split into two parts: (i) the storm-time variation, (Dst) (ii) the solar daily disturbance (SD) or disturbance local – time equality D_s . The disturbance field D is given by:

$$D = Dst + D_s$$

and

$$\langle D \rangle = Dst + SD$$

$\langle D \rangle$ is the average D over 24 h.

This has been taken care of and in this work is referred to as disturbance field.

DISCUSSION

The results presented in Figure 1a to i in this study demonstrate that the diurnal variation in H and Z on international disturbed days for all the nine years under study depict that generally, the features are different for each year. One striking feature of the variation is that while S_d of H maintains the positive for the diurnal variation, S_d of Z consistently remains negative, except for the year, 1997 and 1998. Though in 1993, Figure 1d, both S_d of H and Z attained three maxima at early hours, at 02hrUT, 10hr UT and 16hr UT, this is a striking and abnormal situation. For these two years, 1997 and 1998, it could be seen that both S_d of H and Z continued to be zero until about 18 to 22 h UT and approximately at 14 to 16 h UT respectively. This is another striking and abnormal feature. This could be attributed to the modification of wind and ionospheric conductivity, an observation that is at invariance with the result of Onwumechili (1959).

The average monthly S_d variations for both S_d of H and Z from 1990 to 1998 (Figure 2a to i) show that both variation in H and Z are similar in pattern, still H maintaining positive, while Z negative in most cases, indication that the cause of variation is likely to be from different sources. Except for Figure 2c and h (1992 and

Table 1. Sd variations for H component.

Time	Year								
	1990	1991	1992	1993	1994	1995	1996	1997	1998
0	- 08.00	- 12.00	- 42.00	- 121.00	- 03.00	- 05.00	00.00	- 05.00	- 05.00
1	08.00	12.00	42.00	121.00	03.00	05.00	00.00	05.00	05.00
2	02.00	03.00	- 115.00	02.00	00.00	01.00	01.00	03.00	02.00
3	01.00	00.00	- 119.00	03.00	- 01.00	00.00	00.00	00.00	- 01.00
4	04.00	02.00	- 118.00	03.00	02.00	02.00	- 01.00	00.00	- 04.00
5	07.00	09.00	- 176.00	02.00	04.00	03.00	02.00	- 02.00	- 07.00
6	09.00	08.00	- 163.00	04.00	03.00	03.00	05.00	00.00	- 03.00
7	10.00	04.00	- 120.00	02.00	08.00	05.00	08.00	03.00	- 01.00
8	10.00	- 01.00	- 121.00	- 36.00	07.00	09.00	09.00	04.00	00.00
9	08.00	01.00	- 119.00	124.00	08.00	09.00	12.00	05.00	05.00
10	11.00	04.00	- 119.00	06.00	12.00	13.00	11.00	07.00	08.00
11	11.00	07.00	- 116.00	08.00	14.00	13.00	12.00	08.00	10.00
12	11.00	11.00	- 113.00	10.00	14.00	14.00	13.00	10.00	10.00
13	12.00	07.00	- 162.00	13.00	15.00	14.00	14.00	12.00	10.00
14	02.00	- 08.00	- 115.00	- 35.00	04.00	04.00	07.00	04.00	158.00
15	- 11.00	- 23.00	- 163.00	114.00	- 01.00	- 05.00	- 03.00	- 04.00	- 10.00
16	- 21.00	- 35.00	- 53.00	- 12.00	- 09.00	- 11.00	- 09.00	- 11.00	- 19.00
17	- 29.00	- 45.00	- 25.00	- 13.00	- 15.00	- 14.00	- 10.00	- 14.00	- 22.00
18	- 31.00	- 42.00	- 128.00	- 12.00	- 15.00	- 12.00	- 09.00	- 14.00	- 20.00
19	- 30.00	- 37.00	- 171.00	- 51.00	- 11.00	- 10.00	- 06.00	252.00	- 19.00
20	- 24.00	- 30.00	113.00	- 45.00	- 07.00	- 07.00	- 02.00	256.00	- 12.00
21	- 14.00	- 20.00	- 37.00	00.00	- 03.00	- 04.00	00.00	- 07.00	- 07.00
22	- 07.00	- 07.00	05.00	03.00	- 02.00	- 03.00	- 01.00	- 06.00	- 04.00
23	- 03.00	- 08.00	52.00	03.00	- 01.00	- 02.00	00.00	- 03.00	- 03.00

Table 2. Sd variations for Z component.

Time	Year								
	1990	1991	1992	1993	1994	1995	1996	1997	1998
0	- 03.00	06.00	- 39.00	- 119.00	- 03.00	00.00	- 01.00	00.00	- 01.00
1	03.00	- 06.00	39.00	119.00	03.00	00.00	01.00	00.00	01.00
2	03.00	- 02.00	- 52.00	01.00	03.00	01.00	01.00	01.00	01.00
3	01.00	- 01.00	03.00	00.00	01.00	01.00	01.00	02.00	03.00
4	01.00	- 05.00	04.00	- 01.00	00.00	00.00	01.00	01.00	03.00
5	- 01.00	- 09.00	- 50.00	- 03.00	- 05.00	- 02.00	00.00	00.00	00.00
6	- 03.00	- 16.00	- 42.00	- 07.00	- 08.00	- 05.00	- 03.00	- 03.00	- 06.00
7	- 06.00	- 24.00	- 09.00	- 11.00	- 14.00	- 09.00	- 05.00	- 05.00	- 12.00
8	- 11.00	- 30.00	- 11.00	- 55.00	- 19.00	- 13.00	- 07.00	- 07.00	- 15.00
9	- 13.00	- 34.00	- 13.00	101.00	- 24.00	- 12.00	- 09.00	- 09.00	- 17.00
10	- 18.00	- 39.00	- 18.00	- 17.00	- 26.00	- 16.00	- 10.00	- 09.00	- 23.00
11	- 21.00	- 42.00	- 16.00	- 15.00	- 28.00	- 18.00	- 10.00	- 11.00	- 25.00
12	- 19.00	- 43.00	- 14.00	- 13.00	- 28.00	- 18.00	- 09.00	- 12.00	- 26.00
13	- 10.00	- 45.00	- 65.00	- 09.00	- 25.00	- 17.00	- 08.00	- 12.00	- 24.00
14	- 19.00	- 41.00	- 01.00	- 46.00	- 22.00	- 17.00	- 08.00	- 11.00	138.00
15	- 24.00	- 42.00	- 39.00	110.00	- 23.00	- 19.00	- 10.00	- 13.00	- 21.00
16	- 31.00	- 44.00	78.00	- 12.00	- 26.00	- 22.00	- 16.00	- 17.00	- 24.00
17	- 36.00	- 44.00	102.00	- 15.00	- 27.00	- 25.00	- 19.00	- 20.00	- 26.00
18	- 36.00	- 39.00	- 06.00	- 15.00	- 26.00	- 23.00	- 19.00	- 20.00	- 23.00
19	- 34.00	- 31.00	- 82.00	- 51.00	- 22.00	- 19.00	- 15.00	- 16.00	- 19.00

Table 2. Contd.

20	- 26.00	- 20.00	159.00	- 46.00	- 16.00	- 13.00	- 11.00	- 11.00	- 13.00
21	- 16.00	- 10.00	06.00	- 01.00	- 11.00	- 08.00	- 06.00	- 06.00	- 07.00
22	- 07.00	02.00	49.00	05.00	- 06.00	- 03.00	- 02.00	- 01.00	- 03.00
23	00.00	06.00	119.00	12.00	00.00	01.00	00.00	01.00	01.00

Table 3. Average monthly S_d variations for H and Z components for the years 1990 to 1998.

Year	Months											
	JAN	FEB	MAR.	APR.	MAY	JUN.	JUL.	AUG.	SEP.	OCT	NOV	DEC
1990H	06.00	14.00	09.00	- 25.00	- 09.00	- 12.00	00.00	- 09.00	- 06.00	03.00	- 03.00	- 02.00
1990Z	-02.00	- 10.00	- 29.00	- 39.00	- 25.00	- 28.00	00.00	- 09.00	- 09.00	- 11.00	- 03.00	- 02.00
1991H	00.00	09.00	- 17.00	- 10.00	- 12.00	- 41.00	- 29.00	- 10.00	- 01.00	06.00	01.00	09.00
1991Z	00.00	- 04.00	- 40.00	- 23.00	- 18.00	- 40.00	- 41.00	- 26.00	- 19.00	- 31.00	- 41.00	- 07.00
1992H	- 1004.00	- 21.00	- 05.00	16.00	- 15.00	40.00	08.00	12.00	- 91.00	76.00	- 02.00	- 77.00
1992Z	149.00	- 16.00	07.00	05.00	- 04.00	45.00	00.00	07.00	- 84.00	76.00	03.00	116.00
1993H	105.00	- 07.00	- 46.00	39.00	00.00	01.00	00.00	02.00	- 01.00	- 04.00	04.00	06.00
1993Z	105.00	- 01.00	- 36.00	38.00	05.00	01.00	- 13.00	- 22.00	- 20.00	- 10.00	- 15.00	- 15.00
1994H	01.00	11.00	07.00	00.00	00.00	06.00	05.00	06.00	- 06.00	- 04.00	- 09.00	- 02.00
1994Z	- 04.00	- 29.00	- 12.00	- 34.00	- 22.00	- 12.00	- 17.00	- 10.00	- 11.00	- 16.00	- 09.00	- 05.00
1995H	04.00	08.00	07.00	- 07.00	- 04.00	- 04.00	10.00	- 01.00	- 04.00	06.00	00.00	- 02.00
1995Z	- 06.00	- 08.00	- 13.00	- 11.00	- 19.00	- 14.00	- 12.00	- 10.00	- 14.00	- 14.00	- 07.00	- 05.00
1996H	- 01.00	01.00	09.00	04.00	00.00	- 02.00	01.00	- 01.00	07.00	07.00	03.00	00.00
1996Z	- 04.00	- 04.00	- 08.00	- 11.00	- 09.00	- 07.00	- 08.00	- 09.00	- 09.00	- 05.00	- 05.00	- 04.00
1997H	- 07.00	09.00	06.00	05.00	00.00	- 04.00	- 05.00	- 06.00	- 02.00	04.00	269.00	- 01.00
1997Z	- 06.00	- 09.00	- 07.00	- 10.00	- 15.00	- 11.00	- 06.00	- 07.00	- 08.00	- 09.00	- 02.00	- 04.00
1998H	- 01.00	15.00	05.00	80.00	- 08.00	- 01.00	- 04.00	- 16.00	- 11.00	- 07.00	- 08.00	- 05.00
1998Z	- 03.00	- 09.00	- 11.00	75.00	- 22.00	- 12.00	- 11.00	- 34.00	- 14.00	- 07.00	- 20.00	- 05.00

Tables 1, 2 and 3 depict S_d variations of H component, S_d variations for the Z components and average monthly S_d variation for H and Z components for the year 1990 to 1998.

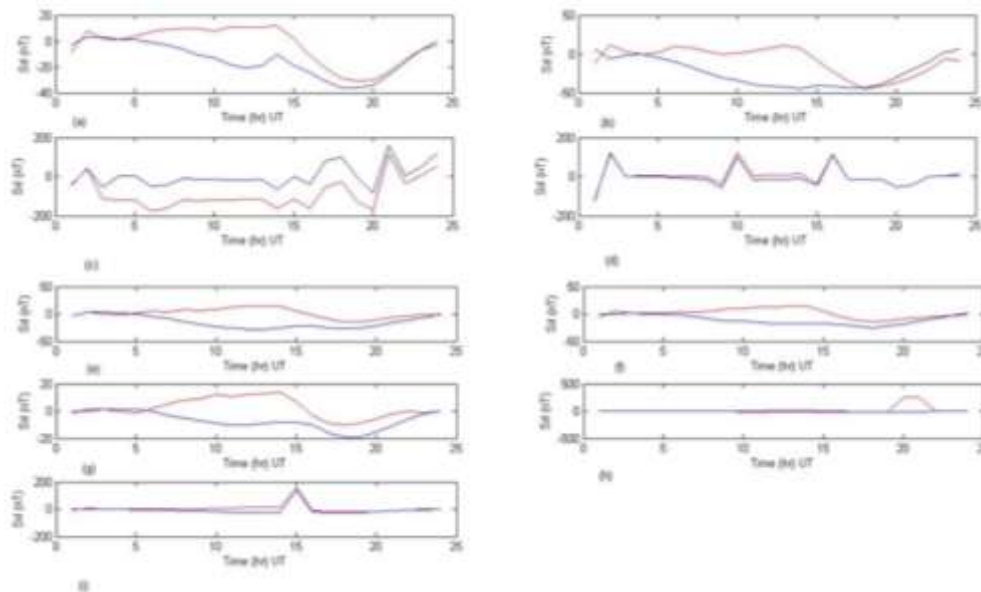


Figure 1 (a-i). S_d diurnal variations for H and Z components from 1990-1998.

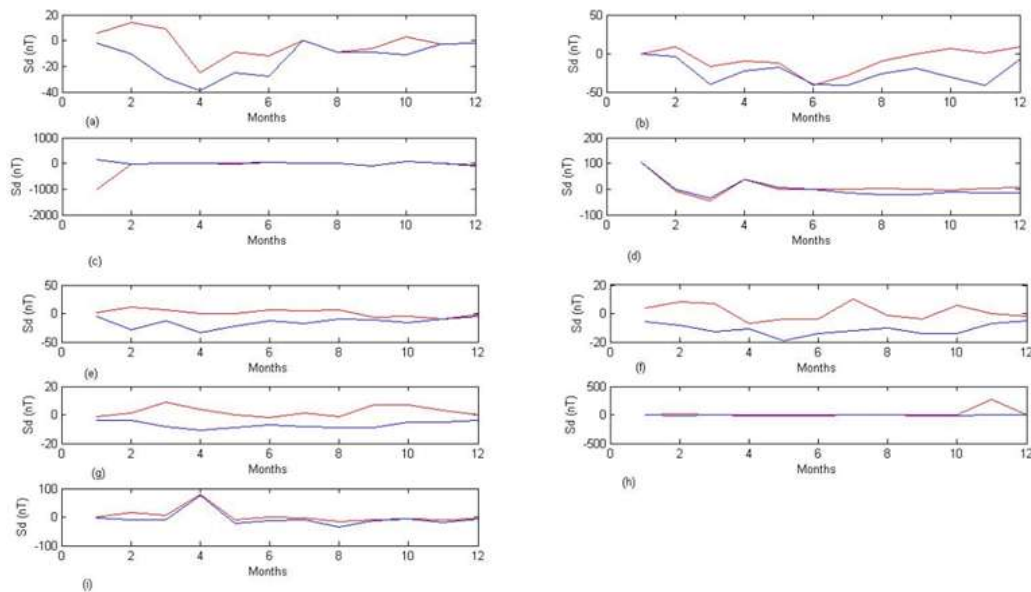


Figure 2 (a-i). Average monthly Sd variations for H and Z components from 1990-1998.

1997) depict very different pattern of variation in both, particularly in 1997 in both Figures 1h and 2h, the same horizontal line along zero is observed. This could be due to extra galactic origin. This year 1997 could be regarded as an abnormal year that requires a further research work for more robust deduction. This could lead to investigation on the relationship between cosmic rays and geomagnetic field variations that invariably will contribute to causes of climate change.

Conclusion

Results of our analysis are compared with those carried out around the dip equator. The comparison confirms that the variation of H and Z components in mid latitudes as compared with the equatorial region is in contrast. The reason being that those in the equatorial electrojet regions come from the same source while those of the mid latitudes are from different sources. It is deduced that the daily diurnal variation of SD horizontal intensity at this mid latitude could be equally attributed to decrease of the ambient field during the night rather than the increase during the day.

Conflict of Interests

The authors have not declared any conflict of interests.

REFERENCES

- Bhargava BN, Yacob A (1971). Depression in the low-latitude horizontal intensity due to quiet-time ring current. *Pure Appl. Geophys.* 92(1):165-168.
- Fambitakoye O (1971). Variabilite' jour-a'-jour de la variation journalie're reguiliere du champ magnetique terrestre dans la region de l'e'lectrojet e'quatorial. *C. R. Acad. Sci. Paris* 272:637-640.
- Jean-Louis Z, Frederic O, Mazaudier CA (2013). Solar activity, solar wind and geomagnetic signatures. *Atmos. Clim. Sci.* 3:610-617.
- Messanga EH, Kosh DCM, Mbane BC (2014). Day-to-Day Variability of H Component of geomagnetic field in Central African Sector provided by Yaounde - Cameroon Amber Station. *Int. J. Geosci.* 5:1190-1205.
- Okeke FN, Hamano Y (2000). Daily variations of geomagnetic H D and Z-field at equatorial latitudes. *Earth Planets Space* 52:237-243.
- Onwumechili CA (1959). The relation between H- Z- variations near the equatorial electrojet. *J. Atmos. Terr. Phys.* 16:274-282.
- Rastogi RG (2006). Magnetic Storm effects at EEJ stations. *Earth Planet Space* 58:1-13.
- Sarabhai V, Nair KN (1969). Daily variation of the geomagnetic field and the deformation of the magnetosphere. *Nature* 223:603-604.
- Vestine EH (1947). The geomagnetic field, its description and analysis, Carnegie Inst. Publ. 580, Washington DC.
- Vonlland H, Taubenheim J (1958). On the ionospheric current system of the geomagnetic solar flare effect (s.f.e). *J. Atmos. Terr. Phys.* 12:258-265.

International Journal of Physical Sciences

Related Journals Published by Academic Journals

- *African Journal of Pure and Applied Chemistry*
- *Journal of Internet and Information Systems*
- *Journal of Geology and Mining Research*
- *Journal of Oceanography and Marine Science*
- *Journal of Environmental Chemistry and Ecotoxicology*
- *Journal of Petroleum Technology and Alternative Fuels*

academicJournals